Adaptive Neuro-Fuzzy Inference System and Artificial Neural Network Modeling for the Adsorption of Methylene Blue by Novel Adsorbent in a Fixed - Bed Column Method

Anbazhagan, Sivaprakasam; Thiruvengadam, Venugopal*[+]; Kulanthai, Kannan

Department of Chemistry, GCE, Anna University, Salem-636011, Tamil Nadu, INDIA

ABSTRACT: *A column study for the removal of Methylene Blue (MB) by the activated carbon from the leaves of Calotropis Gigantea (CGLAC) was done. The CGLAC was characterized by SEM, FT-IR, Raman, TGA/DTA EDAX, BET, and XPS. TGA/DTA studies of CGLAC showed a high fixed carbon content, which indicated that the activated carbon was highly efficient for adsorption. XPS studies confirmed the presence of the aromatic conjugated pi system, C = O and C = C as the main functional group in CGLAC. The pH_{pzc} studies showed that CGLAC has a negative surface charge density and hence adsorption of the cationic dye would be highly efficient. In the column studies, the effect of the parameters like initial concentration (100 – 500 mg /L) of dye, bed height (1, 1.5, and 2 cm), pH (2, 6.5, and 10), flow rate (3.5, 5, and 6.5 mL), and temperature (303, 318 and 333 K) for the removal of MB were tested. Dynamic column models were tested for BTC and it was found that BDST model fitted the experimental data most. R^2 for BDST model was found to be greater than 0.99 for most of the parameters studied. Other models were found to fit BTC model at certain conditions. Higher flow rate showed a better fit towards Thomas model with R^2 value of 0.95. The highest % of removal of MB by CGLAC was found to be 86.4 % for 3.5 ml min^{-1} flow rate, 100 mg/L concentration, and 2 cm bed height. ANN and ANFIS predictive models were applied to the study and both the models were found to give good results. ANFIS model showed the highest R^2 value for validation data compared to ANN and hence ANFIS could be applied to the prediction of adsorption compared to ANN for the column studies.*

KEYWORDS: *CGLAC; fixed-bed column model; BDST; BTC; Artificial Neural Network; Adaptive - Fuzzy Network.*

INTRODUCTION

Pollution of water by the extensive usage of dyes and dye products is one of the major environmental threats to the mankind [1-3]. Dyes cause various problems to the mankind by contaminating water and are a potent carcinogen. Dyes are non-biodegradable, mutagenic and carcinogenic and are not degraded easily in the environment [4,5]. Textile industry is one of the major contributors to the pollution of dye in water; many other industries like paint,

* *To whom correspondence should be addressed.*

+ *E-mail*: *venupaper@gmail.com*

1021-9986/2020/6/75-93 *19/$/6.09*

paper, and food industries also contribute to the pollution of water [6-9]. A textile industry may contaminate water from 2 to 5 mg L^{-1} with a dye. Wide usage of cationic dye in textile, paper and other industries were found to be one of the main contaminants in the water [10, 11]. Many techniques have been used to remove the MB from water, namely; coagulation, photolytic degradation by nano-particle, usage of nano-composite, electro kinetic method, filtration, ion exchange methods and reverse osmosis process [12, 13]. But most of the method suffers from various disadvantages especially they cannot be applied to a large amount of wastewater and are not cost effective (especially nano-particles and nano-composites) and they may cause secondary pollution [14]. This may lead to secondary treatment of water to remove the unwanted secondary material. Many low-cost adsorbents were used to remove Methylene Blue (MB) from the wastewater which includes agricultural wastes like rice husk, peanut shell, industrial wastes like coir waste, and mine industries wastes. These materials have a disadvantage of poor removal of dye and the time taken for removal was found to be too long [15-18]**.** Continuous flow model (Column method) is considered as the main method for the removal of dyes from the industrial wastewater. This work focuses on synthesis of low cost activated carbon from *Calotropis Gigantea* leaves and the usage of activated carbon column to remove MB from wastewater. Column method was chosen for this experimental work so that a new and cost effective reactor can be built to remove the methylene blue from industrial wastewater. *Calotropis Gigantea* leaves has no economic value and could be found in the waste land of South India. Activated carbon prepared from *Calotropis Gigantea* leaves was found to remove a large amount of MB from synthetic water. A small column was found to be very efficient as it removed a higher amount of dye when compared to the other adsorbent. The efficiency of the column was tested under various conditions viz., pH, temperature, bed height, flow rate, and dye concentration. Thomas [19], Adams-Bohart, Wolbroska, Yoon-Nelson [20] and Bed Depth Service Time (BDST) models [21] were used to test the column performance. Artificial Neural Network (ANN) method was used to predict the removal percentage. A thorough review of literature has shown that much work has not been done for predicting the removal percentage using ANN. The Adaptive Neuro Fuzzy Inferences System (ANFIS) which was not used for predicting the column removal efficiency in the other research papers (to the best of author knowledge) was used to predict the removal efficiency of MB by activated carbon in this work.

EXPERIMENTAL SECTION

Adsorbent

Calotropis Gigantea leaves were obtained near Government College of Engineering, Salem, Tamilnadu. These leaves were first cleaned with water, dried in shadow for 5 days, cut into pieces and then powdered. The powdered leaves were then sieved with 100 micron size and were taken for the preparation of the activated carbon. 25 g of powdered leaves were mixed with 50 mL of concentrated sulfuric acid and the mixture was heated to 160^{o} C in an open furnace. The mixture was then cooled and washed with water and 1 % NaOH to remove excess of sulphuric acid present until the pH of the filtrate is neutral. The mixture was then dried at 105^{o} C in an air oven. The dried powdered was preserved at room temperature for further analysis.

Adsorbate

MB was obtained from Sigma-Aldrich Corporation, USA. A stock solution of 1000 mg/L was prepared by dissolving 1g of MB in 1L of double distilled water (DDW). From the stock solution, various concentrations of MB were prepared by appropriate dilution using DDW. The pH of the dye solution was adjusted with 1M NaOH and 1M of HCl.

Method

The column was prepared using a borosil glass column of internal diameter 1cm and a height of 15 cm. The two ends of the column were packed with cotton so that the fixed column cannot be disturbed during the analysis. A mass of 0.25 g was taken to fill the column with a height of 1cm and in this analysis three different heights viz., 1 cm, 1.5 cm, and 2 cm were used. A peristaltic pump was used to give a constant flow of synthetic wastewater at a rate of 3.5 ml/min, 5 ml/min, and 6.5 ml min^{-1}. The schematic diagram of the experimental set up is represented in Fig 1.

Characterization of the Adsorbent

Characterization of the adsorbent was carried out using FT- IR and SEM-EDAX. SEM images of the CGLAC

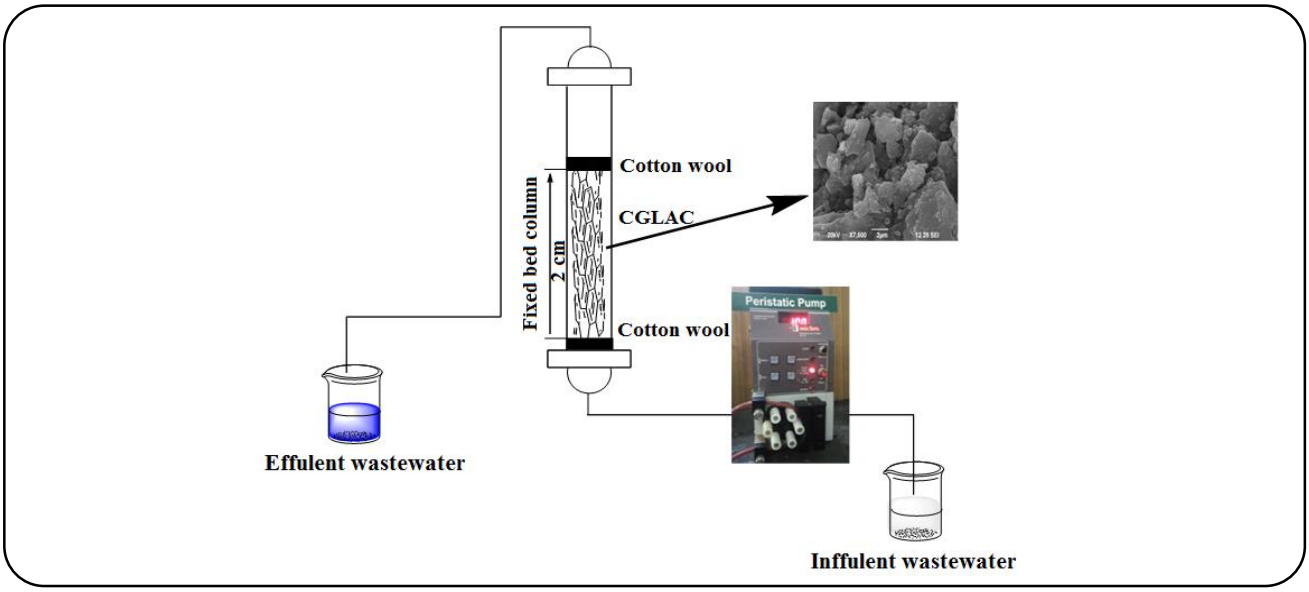

Fig. 1: Schematic diagram of fixed bed column.

before adsorption and after adsorption were shown in Fig. 2(a, b). From the SEM images, it can be easily inferred that after adsorption, the coarse nature of the activated carbon had been reduced. EDAX images have given the elemental composition present in the CGLAC before and after adsorption. Fig. 2 (c) shows that the main elemental compositions of the CGLAC were carbon (C), calcium (Ca), sulfur (S) and oxygen (O). From the EDAX images, the presence of extra sulfur peak (2.18 %) was seen due to the adsorption of the MB onto activated carbon, whereas, before adsorption, the above peak was not seen in CGLAC.

The FT- IR spectrum before adsorption and after adsorption was shown in Fig. 3 (a and b). From the spectrum, it can be inferred that the activated carbon showed a broad peak at around 3200 cm^{-1} which indicated that the presence of OH group either phenolic or alcoholic. Apart from this peak, the activated carbon does not show any appreciable peak in the characteristic functional group area except for a broad peak at around 1500 cm^{-1} which might be owing to the presence of aryl group. After adsorption, peaks (2800 cm^{-1}) are slightly sifted from their position and intensity got altered, due to the weak van-der walls force of attraction between MB ions and the functional group present in the CGLAC. The result indicated that the physical adsorption process. Increase in peak intensity at around 1500 cm^{-1} might be due to the presence of the strong aromatic group in MB.

XRD analysis

Fig. 4 shows the X- Ray Diffraction (XRD) pattern of CGLAC, which confirmed the amorphous nature of the activated carbon. XRD pattern shows two broad peak one at around 23^o which indicated the presence of 002 plane due to disordered graphite. Another broad peak at 43^o indicated the reflective 100 plane. The XRD patterns clearly demonstrate that the lignocelluloses have been destroyed in the carbon matrix [22-24]. The XRD image clearly indicated that the activation of sulfuric acid on the leaves was complete.

Point of Zero Charge (pH_{pzc}) of CGLAC

The pH_{pzc} was found out for CGLAC using solid addition method. In this method, 50mL from 0.01M $NaNO_3$ was transferred to the 100 mL beaker. 10 such beakers were used and the pH of the solution in the beaker was varied from 2 to 12 using diluted HCl and NaOH. 0.125 g of CGLAC was then added to each beaker and placed stagnant without disturbing for 12 hours at room temperature. Final pH of each beaker was then measured and the difference between initial and final pH was calculated [25-27]. The procedure was repeated for 3 times and average values were taken for analysis. Initial pH vs ΔpH was plotted (Fig. 5) to find pH_{pzc}. pH_{pzc} gave an idea of surface coverage, presence of ionic site and active functional group in CGLAC. From the Fig. 5, it can be ascertained that CGLAC has a net negative charge and hence, it can be used to adsorb a positively charged (cationic) dye like MB.

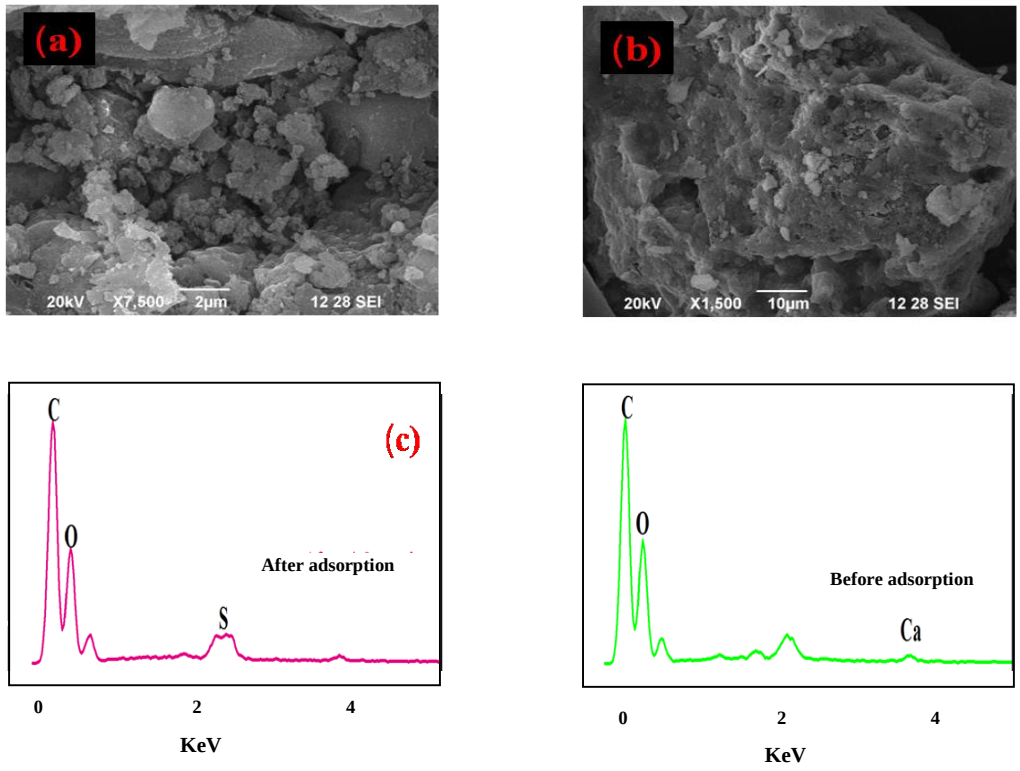

Fig. 2: The SEM pictures (a, b), EDAX (c) showed that before and after adsorption of CGLAC.

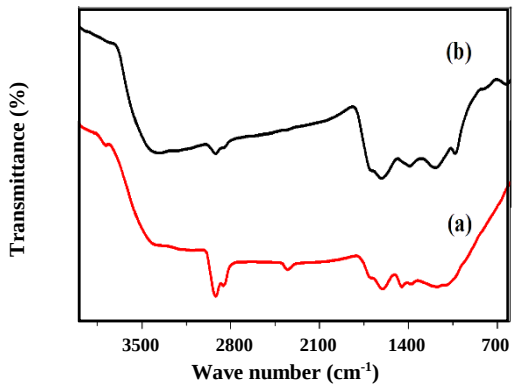

Fig. 3: FT- IR images showed that the before (a) and after adsorption (b) of CGLAC.

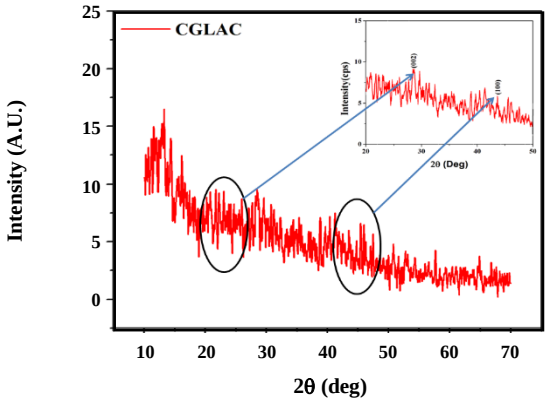

Fig. 4: XRD pattern of CGLAC.

Textural parameters of CGLAC

Surface area and porosity of CGLAC was investigated by BET (Brunauer –Emmett- Teller), which was carried out by standard N_2 gas absorption /desorption isotherm method. The sample was degassed at 450 ^oC for 12 h and BET analysis was carried out. Investigation of surface area was an essential factor for the choice of adsorbent. The adsorbent having high surface area had large binding sites to the adsorbate. Surface area of the activated carbon determined by N_2 - gas adsorption / desorption isotherm analysis was shown in Fig. 6. BET analysis showed that the adsorbent surface area was 15.393 m^2/g. It indicated

Table 1: BET parameters of the CGLAC.

Physical parameters (BET)	Value
Surface area	15.393 m^2/g
Specific surface area	0.410716 m^2/g
Porosity	0.19067
Pore volume	0.06 cc/g
Density	0.808 cc/g
Radius	18.082 A°

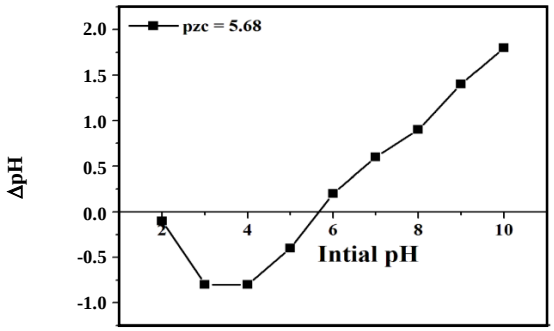

Fig. 5: Point of zero charge of CGLAC.

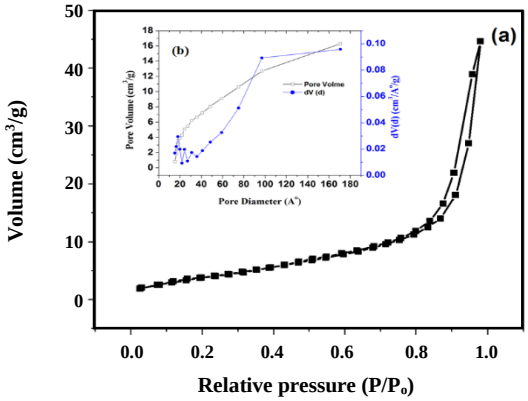

Fig. 6: N_2 adsorption/ desorption isotherm of CGLAC..

that the surface area is large for the accumulation of dye in solution [28, 29]. Fig. 6 indicated the adsorption followed Type - III and it indicated that there was no limiting adsorption even at high pi/p_0. Type - III curve indicated there was a weak interaction between adsorbate and adsorbent. Hysteresis loop of Type - III indicated that the adsorbent CGLAC existed as non-rigid aggregates and has a plate like particle shape. The volume porosity and diameter of the adsorbent were shown in Table 1.

Raman Analysis

A Raman spectra was an important complementary tool to IR spectroscopy and the groups which were IR inactive could be active in the Raman spectra for the activated carbon. A Raman spectrum of the carbonaceous materials does not give many peaks, but the intensity of these peaks might give much valuable information about the structure of the carbon. It might give important insight to the physical characteristic of the activated carbon like size, disorderliness of the microcrystalline carbon network [28-30]. In Fig. 7, the Raman spectra of CGLAC show two broad peaks at around 1380 cm^{-1} and 1670 cm^{-1}. The peak at 1670 cm^{-1} also known as G band arises due to the vibration of sp^2 hybridized graphite like hexagonal structure of the graphite. The disordered sp^3 hybridized carbon showed the peak at 1380 cm^{-1} (D band) which in turn indicated that the micro porous and amorphous structure of carbonaceous substance [29]. The D/G peak intensity ratio gave a measure of the degree of graphitization during the activation process. Higher the D/G ratio would mean lower graphitization. CGLAC showed a D/G ratio of 1.09 which indicated lower graphitization during the activation process. Lower graphitization resulted in introduction of micro pores into the activated carbon which led to the increase in defects and disorders which in turn led to amorphous nature [30-32]. The Raman spectra clearly confirmed that the CGLAC was highly amorphous and has micro porous structure.

XPS Analysis

XPS spectrum of CGLAC was showed in Fig.8 (a, b). These spectra showed valuable information of the functional group present in CGLAC. The binding energy and peak intensity of the peak showed information about the nature and the relative abundance of the functional group. High intensity peak at lower binding energy in the carbon 1s showed that the presence of C = C conjugated system with aromatic rings. FT-IR analysis also confirmed the presence of the aromatic group. XPS of CGLAC showed a carbon 1s electron peak at around 284.34 eV that corresponded to graphitic C - C and carbon peak at 285.52 eV that corresponded to C - O peak and another peak at 286.45 eV that corresponded to C = C group [33, 34]. XPS spectra confirmed the presence of these groups which was also shown by FT-IR. Various functional groups present in the CGLAC were given in the Table 2. O 1s peaks

Table 2: Chemical analysis of CGLAC determined by XPS.

S.No	Signals	Peak (eV)	Assignment
1	C 1s	~ 284.34 ~ 285.52 ~ 286.42	Graphite, Ar- C C-OH C = O, C-NH_2 and C≡N group
2	O 1s	~ 530.41 ~ 530.0 ~ 533.2	-COOH (Carboxylic group) -C = O (Carbonyl group) -C-OH (Hyroxyl group)

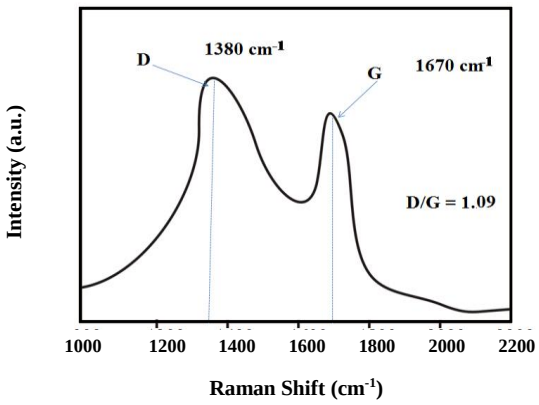

Fig. 7: Raman Spectra of CGLAC.

confirms the presence of the major functional group like C = O, C - O, amide and alcohol functional group. The absence of sulfur peak confirmed that there was no sulfuric acid or sulfate residue present in CGLAC and hence, washing was complete as discussed earlier.

Proximate analysis of CGLAC was represented in the Table 3. The analysis confirmed that CGLAC showed a very low ash content. Fixed carbon and ash content of CGLAC were found be around 75 % and 3 %. The low ash content and high carbon content indicated that the activation of CGLAC was efficient. The sulfuric acid activation of the CGLAC has degraded most of the organic substance and has been discharged as gases during the activation process. As a result, a high fixed carbon was present in CGLAC which was responsible for high efficiency of the carbon mass for the removal of MB. Different methods of activation of *Calotropis Gigantea* leaves viz., pyrolysis, base (KOH) activation were done using the standard procedure from the literature. It was found from proximate analysis that the fixed carbon content for those activations were low. Hence, these activated carbons were not efficient in the removal of the dye. TGA-DTA analysis of the CGLAC was shown in Fig 9. The analysis was carried out in N_2 atmosphere to find out the thermal stability of the activated carbon. Many authors have used TGA-DTA analysis to determine the presence of the hygroscopic groups and other functional groups present in the activated carbon [35, 36]. TGA-DTA analysis showed three mass loss steps, at around 100, 450° and 550 °C respectively. The first mass loss of around 10 % was due to the loss of physically adsorbed water. This water might be due to the physical absorption during the storage process of CGLAC. The presence of the hygroscopic functional group might have caused the attraction of water from the atmosphere through hydrogen bonding. The Oxygenated surface in the activated carbon could form hydrogen bond with water [37]. The second and third mass loss region in the sample indicated oxidative degradation of the functional group present in the activated carbon. The loss in weight of the carbon mainly occurred owing to the oxidation of the groups into CO and CO_2 as gases. The second mass loss at around 400 to 500 °C was due to the oxidative degradation of the functional groups which were less thermally stable. In this temperature range carboxylic acid derivatives like carboxylic acids, anhydrides and lactones were decomposed since they were less thermally stable [38-40]. The third mass loss step could be attributed due to the decomposition of phenols, quinines, hydroquinone and other thermally stable functional group. DTA in addition to the three peaks showed a peak at around 600 °C which might be owing to the degradation of the carbon skeleton in the activated carbon. It can be seen from the TGA-DTA curve that the residue content was very low which indicated that there was no silicon or aluminum present as residue.

Theoretical background

The real usage of activated carbon from *Calotropis Gigantea* leaves could be determined by studying the shape of "Break through the curve" (BTC) in a fixed bed column condition and the break point appearance. BTC represented a plot of effluent dye concentration versus lapse time [41]. The adsorption performance of the activated

Table 3: Proximate analysis and elemental analysis of the CGLAC.

Adsorbent	Proximate analysis				Ultimate Analysis		
CGLAC	Moisture (%)	Volatile matter (%)	Fixed carbon (%)	Ash content (%)	% C	% Ca & Mg	% O
	11.52	10.08	75.25	3.12	59.92	1.48 & 0.77	37.83

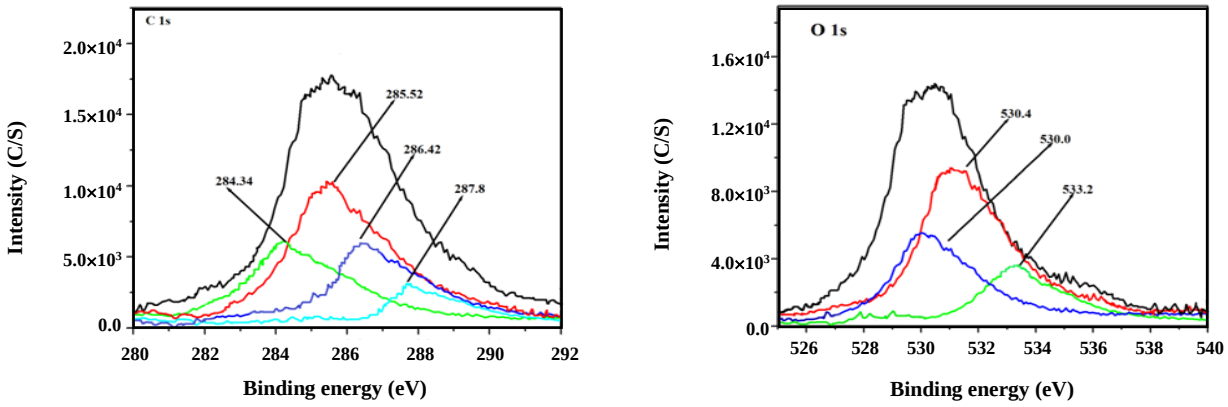

Fig. 8: XPS analysis of CGLAC at (a) C1s, (b) O1s.

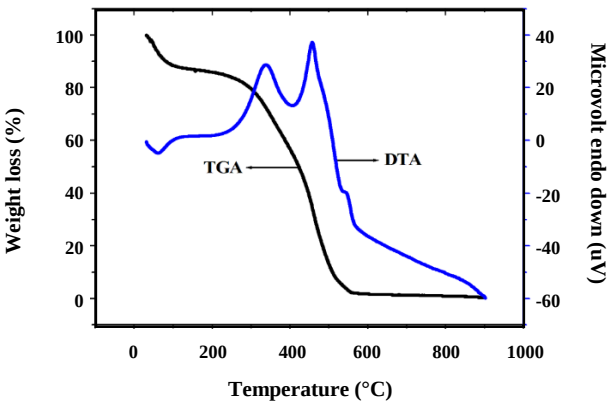

Fig. 9: TGA/DTA analysis of CGLAC.

carbon bed column could be ascertained by breakthrough ($t_{2\%}$) and exhaustion time ($t_{99,5\%}$). The breakthrough point in this study was taken as the time required for the effluent concentration to have 2 % inlet concentration i.e., C = 0.02 C_o. When the effluent concentration has reached 95 % of the original solution i.e., C = 0.95 C_o then exhaustion point was found to be reached. Inlet concentration, flow rate, pH, temperature and bed height were the variables which characterized the shape of the BTC curve. The plot of "$C_{efflunet}$ (C) or $C_{effluent}$ / $C_{influent}$ (C/C_o)" versus "t" showed a typical BTC, for the given bed height, flow rate and concentration of the dye.

The following parameters characterize the column data

$$t_t = \int_{t=0}^{t=\infty} \left(1 - \frac{C}{Co}\right) dt = A_t \quad (1)$$

t_t = Total time

The usable capacity of the column is given by

$$t_u = \int_{t=0}^{t_b} \left(1 - \frac{C}{Co}\right) dt = A_1 \quad (2)$$

t_u = Time equivalent to usable capacity, t_b time taken for C to become 0.02 C_o i.e., breakthrough point.

$t_u \approx t_b$ for most of the column bed studies.

Area of the curve $\int_{t=0}^{t=\infty} \left(1 - \frac{C}{Co}\right) dt$ gives t_t values and $\int_{t=0}^{t_b} \left(1 - \frac{C}{Co}\right) dt$ curve gives t_u. The fraction of total bed capacity utilization upto break point is given by t_u/t_t.

The effective height which was used for adsorption could be represented by Mass Transfer Zone (MTZ) or unused bed height (H_{Un}). Many factors control MTZ namely, temperature, flow rate, solution pH, inlet dye concentration, height of bed, particle size of the activated carbon, adsorbate nature and adsorbate characteristics.

MTZ is given by

$$MTZ = H_{Un} = \left(1 - \frac{t_u}{t_t}\right) H_T \quad (3)$$

H_T is total height of the column in cm

The used bed length H_U may be represented as

$$H_U = \left(\frac{t_u}{t_t}\right) H_T \quad (4)$$

V_{eff} is total effluent volume which is given by

$V_{eff} = Qt_{total}$

Q is volumetric flow rate in ml min^{-1} and t_{total} is total flow in minute.

R % is the total removal percentage of MB dye by the activated carbon. R % could be determined from the ratio of mass of the dye adsorbed (q_{total}) to the overall quantity of the MB dye pumped into the column (m_{total})

$$\%\,R = \frac{q_{total}}{m_{total}} \times 100 \quad (5)$$

The total MB dye adsorbed in the column for a specified bed height, initial dye concentration and flow rate is given by

$$q_{total} = \frac{QC_o}{1000}\int_{t=0}^{t=total}\left(1 - \frac{C}{C_o}\right)dt \quad (6)$$

m_{total}, the total amount of dye sent to the column is given by

$$m_{total} = \frac{CoQt_{total}}{1000} \quad (7)$$

Section area of the column given as *A* cm^2 was calculated from the equation

$$A = 2\pi H_T + 2\pi r^2 \quad (8)$$

Where, H_T is the bed column height and *r* is the inner radius of the column.

Various models describing the column BTC and its usefulness were studied. In this work, five models were used to describe BTC and fitting of the curve against each models.

Adams-Bohart model

This model is one of the most widely used and a simplified form of Thomas model. It was mainly used to predict the initial part of BTC. This model worked on the assumption that there was no inter-particle diffusion and mass transfer external resistance. The adsorption kinetics was considered to be controlled by adsorbent and adsorbate surface chemical reaction. The model also assumed that

i. The fixed bed has practically no axial and radial dispersion

ii. Void fraction in column was constant

iii. The physical property of the adsorbent and adsorbate does not change.

The linear form of Adams - Bohart equation used in this work is given as

$$\ln\left(\frac{C}{C_o}\right) = \frac{LN_oK_{AB}}{U} - K_{AB}C_o \quad (9)$$

K_{AB} is the Adams - Bohart rate constant, N_o is adsorption capacity for the unit volume of the column and *U* is linear velocity of the solution. A plot of $\ln\left(\frac{C}{C_o}\right)$ vs t showed a straight line. Slope and intercept of the line could be used to determine K_{AB} and N_o.

The Wolborska model

This model finds application in the initial part of BTC curve at relatively low concentration of the dye. Axial diffusion of the dye to the activated carbon and external mass transfer was considered to be the main contribution to BTC at relatively low concentration. The linear form of Wolborska model is given by

$$\ln\left(\frac{C}{C_o}\right) = \frac{\beta_a C_o}{N_o}t - \frac{\beta_a L}{U} \quad (10)$$

β_a is kinetic coefficient of external mass transfer where,

$$\beta_a = \frac{U_o}{2D}\left(\sqrt{1 + \frac{4D\beta_o}{U^2}} - 1\right) \quad (11)$$

D is axial diffusion coefficient

Thomas model

One of the most widely used models for determining column performance in predicting BTC was Thomas model. This model mainly followed the Langmuir kinetics of adsorption and assumed that there was a plug flow condition in the column. It also assumed that there is no axial dispersion in the column and second order kinetics were assumed to be the driving force for the adsorption. The main disadvantage of this model was that the adsorption was controlled by second order kinetics and mass transfer at the interface which in turn contributed to the adsorption along with chemical reaction.

The linear form of the Thomas model is given by the equation

$$\ln\left(\frac{C_o}{C} - 1\right) = \frac{K_T q_o}{Q}m - \frac{K_T C_o V_{eff}}{Q} \quad (12)$$

Where, K_T is Thomas rate constant (mL/min.mg), q_o is the predicted equilibrium adsorbate amount in mg/g,

m is for the amount of the activated carbon in gram, V_{eff} is effluent volume, C_o and C are inlet MB and effluent MB concentration and Q is flow rate (mL/min).

$\ln\left(\frac{C_o}{C}-1\right)$ vs t gives linear plot with slope and intercept is used to calculate K_T and q_o

Yoon-Nelson Model

This model was less complicated as it has not been dependent on the characteristics of the dyes and activated carbon used and also not on the physical property of the column bed. Yoon-Nelson model worked on the principle that "the probability of adsorption and breakthrough of dye and activated carbon determined the rate of adsorption on the column of given depth". So adsorption and desorption were considered by Yoon-Nelson model as the determining factor of rate of adsorption in the column.

Yoon-Nelson model is given as linearized equation in the following formula

$$\ln\left(\frac{C}{C_o-C}\right) = K_{YN}t - K_{YN} \quad (13)$$

K_{YN} is *Yoon* and *Nelson* rate constant (min^{-1}). τ is the predicted time for 50 % adsorption in breakthrough curve in (min)

The plot of $\ln\left(\frac{C}{C_o-C}\right)$ vs t results in a straight line and the slope and intercept gives K_{YN} and τ

Bed depth service time (BDST) model

BDST model was also a model widely used for studying the adsorption characteristic in the column study which stated that the column height and service time has a linear relationship. BDST model was derived from Adams-Bohart model which was modified by Hutchins [42]. A process like external mass transfer resistance and intra-particle diffusion was considered to be negligible in the BDST model. BDST model predicted that surface chemical reaction of the solute and the unused adsorbent was used to control the adsorption kinetics.

The linearized form of BDST is given by

$$t = \frac{N_o H_T}{C_o U} - \frac{1}{K_o C_o}\ln\left(\frac{C_o}{C}-1\right) \quad (14)$$

N_o is the adsorption capacity (mg/L), K_o is the rate constant (L/mg.min) H_T is the bed height. Plot of t vs H_T gives a straight line and slope and intercept give N_o and K_o

A more simplified form of the equation is given as

$$t = aH_T + b \quad (15)$$

The slope of the straight line gives a which is given as $a = \frac{N_o}{C_o U}$ and the intercept

$$b = \frac{1}{K_o C_o}\ln\left(\frac{C_o}{C}-1\right) \quad (16)$$

ANN Prediction

The ANN could be used to solve many non-linear problems which use weights and bias from the training method to determine the best fit for the problem. ANN model was based on the biological neural model which was used to predict the percent removal of dye by the column. ANN used the structure which consists of the input layer, a hidden layer and the output layer. Input layer received the data from the independent variable and the data was passed on to the hidden layers through neurons and weighed connections. From the neurons, the data was again carried out to the output layer by the weighed connection. In the ANN modeling, first data was given for training data and then the prediction was made from the other set of data. The model was validated by comparing the results of the trained and predicted data. ANN used weights and bias as the input for each layer and ANN trains the weights and bias in such a way to get the optimum results [43-45].

ANFIS Prediction

ANFIS was another important method to solve the non-linear problem to predict the maximum removal of dye from the wastewater. The method was based on Takagi-Sugeno-Khan (TSK) model [46]. ANFIS could be considered as combination of the human based ANN modeling and the fuzzy rule of if –then. ANFIS could be used to solve where linear method fails and it works on the membership function based on the fuzzy interface system and artificial intelligence based back propagation method [47]. In addition to the membership function and if-then rule, ANFIS also used logical operations to solve the non-linear problem.

RESULTS AND DISCUSSION

The effect of the removal of MB by the CGLAC was studied by BTC curves. The BTC curves were obtained by plotting ratio of outlet concentration of dye to inlet concentration (C/C_o) vs time for different flow rates,

different concentrations, different bed heights, different pH and different temperatures, varying one parameter and keeping other variable constant. It was found that initially, the adsorption of dye towards the column was maximum with increase in time. The saturation of the column occurred and equilibrium was reached between the adsorbed and unadsorbed dye. As a result, the "S" type curve i.e., breakthrough curve was obtained.

Effect of inlet MB Concentration

The inlet concentration of MB was considered as one of the most important limiting factors for the removal of the dye by the column. As the column has fixed mass of activated carbon and the amount of the dye would be the deciding factor for the removal. When the amount of dye was increased then the column would get saturated quickly and a steeper BTC was obtained. So, when the concentration of dye increased, there was a lesser volume of dye solution purified by the column [48]. In this study, removal of MB at various concentrations ranging from 100 mg/L to 500 mg/L at various bed heights were found out and the corresponding BTC curve was plotted. Fig. 10 (a), the temperature, flow rate and pH of the solution were kept constant at 303 K, 3.5 ml min^{-1} and 6.5 respectively. Table S1(S - Available in Supplementary Data) has shown all the parameters for the column adsorption at various concentration and bed height. It can be seen for all the bed heights that the increase in concentration of the dye led to a decrease in the exhaustion time. MTZ was also found to increase which suggested that the saturation has occurred at the faster rate with increase in concentration. BTC showed an increasing trend that when the concentration increased, the BTC became steep. This could be attributed to the fact that when there was an increase in the dye concentration, the active site for adsorption was covered quickly. With the increase in time, the active sites for the adsorption became less [49]. There was no definite trend in the removal percentage when the concentration of the dye solution increased for a given bed height. As the dye concentration was increased from 100 to 200 mg/L, the removal % decreased from 80.58 % to 62.64 % for 1.0 cm bed height, with near 18 % reductions. But when the concentration of dye increased from 200 to 300 mg/L, the removal percentage decreased. With further increase in concentration, the removal percentage was not reduced drastically. This trend was observed for all the bed heights. This property could be mainly attributed to the saturation of the column adsorption site which does not get drastically affected at higher concentration. The shorter saturation period was also confirmed by the value of V_{eff} which was also found to decrease with increase in the concentration. With increase in concentration, higher inter-particulate diffusion may also be a contributing factor for the quicker saturation of the column. And again breakthrough time decreased from 94 minutes for 100 mg/L to 14 minutes for 500 mg/L, with increase in concentration. Similar trend was also seen for the other bed heights.

Effect of column height

The effect of column height for the removal and BTC of the dye on the CGLAC was studied using 3 different column heights viz, 1 cm, 1.5 cm and 2.0 cm at different concentration of the dye. With increase in the bed height, the removal percentage was found to increase and BTC became steeper at exhaustion time as seen in Fig.10 (a), (b), (c). Various parameters for the removal of the dye at different bed height are given in Table S1. Increase in % removal with the increase in bed height suggested that the number of activation site for adsorption increased. The breakthrough time for each bed height was tabulated in the Table S1. From this table, it can be inferred that the breakthrough time nearly doubled for most of the concentration when the height was doubled except for 100 mg/L and showed a lesser increase in the breakthrough time with increase in the bed height. Inter-particulate diffusion and adsorption was slower at lower concentration which led to competitively lower breakthrough time at higher bed depth. From the Table S1, it can be inferred that V_{eff}, height of the column and MTZ increased with the increase in bed height. Although the adsorption site increased when the bed height increased, the ratio of the used to unused site decreased for the higher bed height which might be due to competition of the dye to get adsorbed in the given site [49].

Effect of Flow rate

The effect of flow rate on the adsorption was studied by the flow rate from 3.5 to 6.5 ml min^{-1}, with 100 mg/L dye concentration, 303 K temperature, 1.0 cm bed height and 6.9 pH maintained as constant. For continuous treatment of industrial wastewater, fixed bed column flow

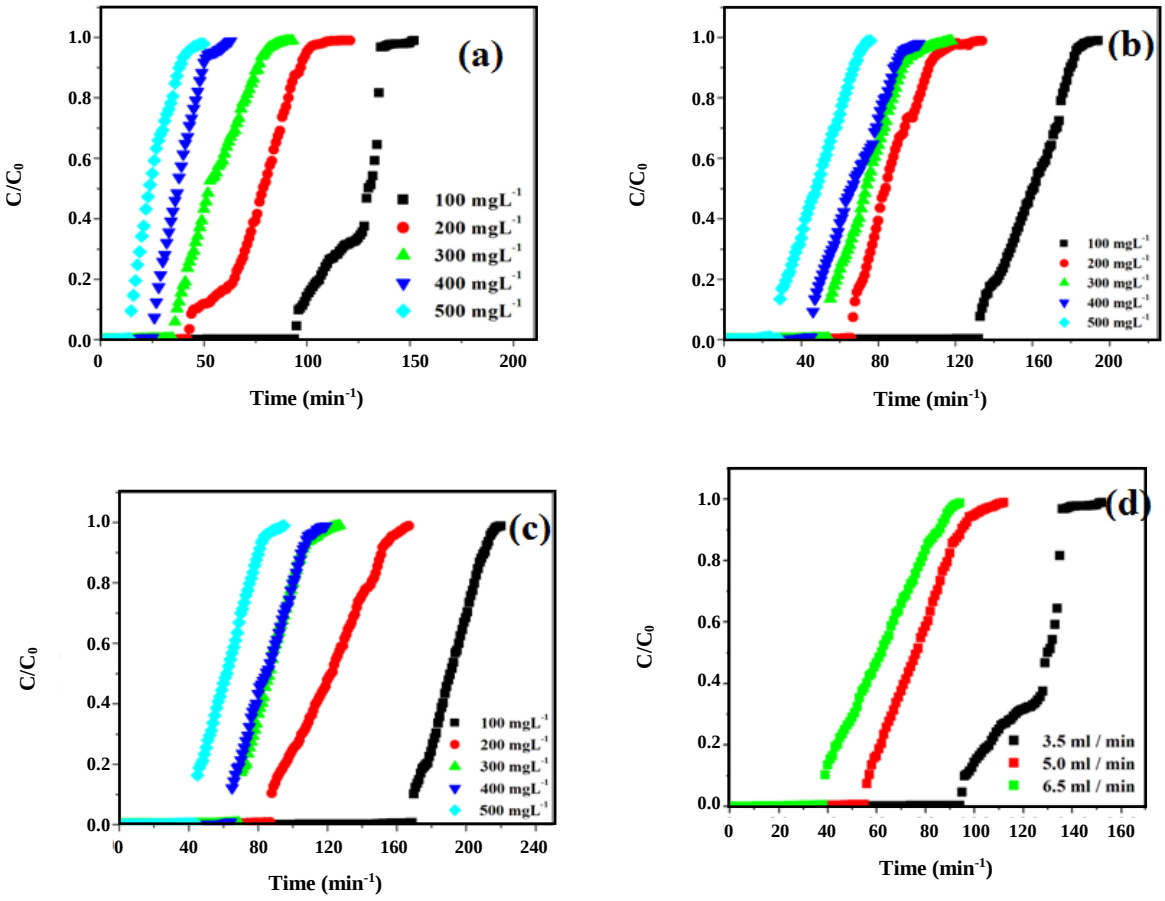

Fig. 10: Plot (a, b, c, d) are BTC for adsorption of MB on CGLAC effect of the MB different concentrations (a), bed height (a, b, c), flow rate (d), at 303 K).

rate played an important role in determining the performance of the adsorption parameter in the column. Table S2 and Fig.10 (d) showed the effect of MB dye adsorption onto CGLAC at various flow rates. It was found that with the increase in the flow rate, the breakthrough time and exhaustion time decreased, the removal efficiency decreased from 80.58 % to 64.71 % and MTZ showed an increase in value. As the flow rate increased, the residential time of the dye in the column decreased. Hence, the probability of the dye getting adsorbed on to the column decreased. This might be attributed to the fact that the dye molecule had no enough time to find the activated carbon to get adsorbed.

Effect of pH

The pH of the solution has an important effect on the adsorption of the dye towards the column with increase or decrease in the pH is the adsorption characteristics could change drastically in the column. The electrical charge on the activated carbon depends on the pH of the solution. The effect of the pH on the percentage removal and BTC was determined by running the column at different pH (2, 6.9 and 10) to characterize the BTC in acidic, neutral and basic medium respectively. Fig. S1 (a) and Table S2 shows the characteristics of the effect of pH on BTC. BTC was found to lie to the left of pH 6.9, but it is far from the left of pH 2 and 10. From the table, it can be inferred that breakthrough time was very less for the solution with pH 2 due to the faster saturation of the column. The experiment suggested that increase or decrease in pH resulted in the decrease in breakthrough time, decrease in % removal, increase in MTZ and decrease in V_{eff} compared to the dye solution at neutral pH. The used column height was found to be highest for the dye

in neutral solution and very low for the acidic solution. The BTC at pH 2 was found to be very steep as the saturation time for the solution with the activated carbon was considerably low. The electrostatic force of attraction and chemical reaction between the dye and adsorbent decided the removal of dye in the column. The reason for the poor removal of the basic dye MB in acidic pH owing to functional group gets protonated in activated carbon [50]. The protonated functional group would have a less electrostatic attraction towards the MB as a basic dye and has a positive charge. So the electrostatic forces of repulsion between the charges would lead to decrease in the % removal and hence, BTC shifted more toward the left. An increase in pH affected the adsorption as the positive charge of the dye would be associated with the hydroxyl ion in the solution. The attraction between the dye and the column would be less compared to the adsorption at neutral pH. So the pH study indicated that the dye could be removed from the neutral solution rather than in the acidic or in the basic pH.

Effect of temperature

The effect of temperature was not normally studied due to the complex instrumental set up, of constant temperature (Temp) was maintained throughout the experiment. In this work, specially designed oven was used to maintain the temperature of the solution. The inlet solution was preheated using an oven and the temperature of the outlet solution was checked to confirm the maintenance of solution temperature. In this experiment, three different temperature were studied viz., 303 K (room temperature), 318 K and 333 K. The Fig. S1 (b) shows the BTC for various temperature and the corresponding data is presented in Table S2. BTC curve was found to move towards the left with the increase in temperature and was found to be steeper at high temperature. From the Table S2, it can be inferred that with the increase in temperature the breakthrough time was found to become less. At 333 K, the breakthrough time was found to be only 8 minutes for 100 mg/L solution at neutral pH and flow rate of 3.5 mL/min. The MTZ was also found to increase with the increase in temperature, which indicated that saturation was achieved quickly when the temperature increased. The results might be explained by considering the fact that the physical adsorption (Electrostatic force of attraction) played an important role in the mechanism of the adsorption. With the increase in temperature, the physical adsorption decreased due to the weakening of electrostatic forces of attraction between the adsorbent and the adsorbate, which led to faster elution of the dye.

Thomas model

Thomas model of fitness for the column was carried out by plotting $\ln\left(\frac{C_o}{C}-1\right)$ vs t, and R^2 was calculated to find the applicability of the model towards the column studies. Table 4 gives the values of R^2, K_{TH} and Q from the straight line fit of the Thomas model. It can be inferred from the table that R^2 value ranges from 0.6 to 0.95. With increase in the flow rate, correlation coefficient (R^2) values increased and this is showed that the Thomas model was fitted the column. K_{TH}, rate constant for Thomas model was found to increase and Q value was found to decrease with the increase in flow rate. With increase in the concentration of the dye solution, it fitted well, K_{TH} decreased, and Q was increased with a change in pH, R^2 and K_{TH} value was increased and Q decreased. With an increase in temperature the R^2 value was first found to decrease drastically and then at 333 K it was increased, K_{TH} value showed an increased and consequently, Q value decreased which indicated that with increase in temperature there was a decrease in adsorption of the dye. Interestingly, it was found that with increase in the bed height the deviation from the Thomas model increased with the lowest R^2 value at the bed height of 2.0 cm in 100 mg L^{-1}. The same trend was observed at higher concentration also, that with increase in bed height, the R^2 value showed a decrease in value. The value of Q decreased with an increase in bed height for the same concentration which showed a poor fit of Thomas model.

Adams-Bohart model

Adams-Bohart model is a modification of Thomas model and Table 4 shows the results of the plot of $\ln\left(\frac{C}{C_o}\right)$vs t. It can be inferred from the table that the Adams-Bohart model was fitted poor, when compared to the Thomas model. R^2 value ranges from 0.56 to 0.89. It was found that R^2 value has not exceeded 0.9 for all the experimental condition which indicated that the Adams-Bohart model fitted poorly to BTC. The results also indicated that the same pattern was followed as the Thomas model, with one exception. When the flow rate

Table 4: The parameters using linear regression analysis and fixed bed column adsorption of MB by CGLAC at different conditions.

S. No	Parameter					Thomas			Adams-Bohart			Yoon Nelson				Wolborska	
	C_0 mg L^{-1}	H_T Cm	Flow rate ml/min	pH	Temp K	K_{TH} ml^{-1} mg L^{-1}	Q	R^2	K_{AB} L mg^{-1} min^{-1}	N_0 mg L^{-1}	R^2	K_{YN} Min^{-1}	τ (min)	50% (exp)	R^2	β_a	N_0
1	100	1	3.5	6.9	303	0.000878	176.51	0.8690	0.00070	10860.1	0.8912	0.08784	126.083	130	0.86905	7.6075	10860.1
		1	5	6.9	303	0.001302	157.14	0.9261	0.00097	10002.7	0.8589	0.13026	78.5710	76	0.92618	9.7827	9998.678
		1	6.5	6.9	303	0.001508	168,36	0.9545	0.00117	10515.8	0.8689	0.15087	64.7525	62	0.95450	12.335	10515.79
		1	3.5	2	303	0.004133	21.52	0.8704	0.00262	1552.95	0.6598	0.41333	25.0491	13	0.87041	3.9988	1522.947
		1	3.5	10	303	0.001535	94.61	0.8827	0.00118	5934.95	0.7635	0.15357	67.5823	66	0.88273	7.00324	5934.001
		1	3.5	6.9	318	0.001718	55.49	0.6413	0.00120	3715.6	0.4763	0.17180	39.6070	37	0.64134	4.46581	3715.631
		1	3.5	6.9	333	0.036416	30.22	0.8023	0.00261	1976.3	0.6209	0.36416	21.5874	18	0.80236	5.66295	2166.145
		1.5	3.5	6.9	303	0.000633	158.9	0.7847	0.00051	7268.51	0.7844	0.06338	170.255	161	0.78472	10.0787	7268.512
		2	3.5	6.9	303	0.000480	157.09	0.6006	0.00040	5635.91	0.5826	0.04804	224.411	193	0.60061	2.28648	5635.910
2	200	1	3.5	6.9	303	0.000654	218.4	0.8858	0.00048	14321.9	0.7913	0.13510	78.4452	79	0.92285	6.94157	14325.82
		1.5	3.5	6.9	303	0.000580	170.25	0.8303	0.00041	8351.05	0.7145	0.11607	91.2115	84	0.83035	3.49658	8350.734
		2	3.5	6.9	303	0.000373	176.13	0.7149	0.00028	6629.15	0.6117	0.07472	125.809	123	0.71493	1.91648	6628.011
3	300	1	3.5	6.9	303	0.000520	249.09	0.8636	0.00036	17427.0	0.7085	0.15608	59.3035	52	0.86346	6.03834	16569.12
		1.5	3.5	6.9	303	0.000407	220.47	0.7774	0.00028	110117	0.6301	0.12226	78.7383	73	0.77744	3.14874	11014.73
		2	3.5	6.9	303	0.000354	193.77	0.6897	0.00025	7809.46	0.5647	0.10623	98.5419	86	0.68979	1.94455	7656.734
4	400	1	3.5	6.9	303	0.000550	227.04	0.8220	0.00038	15167.2	0.6605	0.22036	40.5584	37	0.82220	5.82270	15171.32
		1.5	3.5	6.9	303	0.000338	387	0.7661	0.00025	12596.5	0.6435	0.13529	71.1496	66	0.76611	3.24739	12596.54
		2	3.5	6.9	303	0.000267	253.52	0.6508	0.00020	9753.50	0.5381	0.10718	90.5419	85	0.65087	1.95723	9753.262
5	500	1	3.5	6.9	303	0.000529	206.6	0.8153	0.01035	13700.1	0.6111	0.26488	29.5166	23	0.81530	5.06169	14335.84
		1.5	3.5	6.9	303	0.000324	351.9	0.8109	0.00023	11519.7	0.6607	0.16228	50.2703	48	0.81094	4.03997	17279.60
		2	3.5	6.9	303	0.000291	230.75	0.7183	0.00021	8856.4	0.5750	0.14552	65.9280	62	0.71834	1.90406	9042.863

increased for Thomas model was found to fit the BTC whereas Adams-Bohart model seemed to fit poorly. With the change in pH also the Adams-Bohart model was less followed. K_{AB} and R^2 value has not followed a definite trend in BTC. K_{AB} increased with increase in flow rate but R^2 value decreased when the flow rate was changed from 3.5 ml min^{-1} to 5.0 ml min^{-1} whereas, increases when the flow rate was increased to 6.5 ml min^{-1}. The adsorption capacity N_o was found to increase when the flow rate increased. With the change in pH the adsorption capacity N_o decreased which was in trend with the breakthrough time, whereas increase, in pH also followed the same trend. Bed height changes on BTC showed no definite trend in R^2 and N_o whereas, K_{AB} showed a decrease in value with increase in bed height. Increase in temperature on BTC showed a regular decrease in N_o value and increase in K_{AB} value.

Yoon Nelson Model

Yoon Nelson model was obtained by plotting $\ln\left(\frac{C}{C_o - C}\right)$ vs t. The values of K_{YN}, the rate constant and τ were presented in Table 4. It was found that the removal of MB in the activated carbon, BTC showed a better fit towards the Yoon Nelson model with R^2 ranging from 0.60 to 0.95 for various conditions. It was found that R^2 values increased with the increase in flow rate and also the rate constant K_{YN} was increased whereas, τ the half time or

time for 50 % removal was found to decrease, which was consistent with the experimental data for 50 % removal and was also tabulated in the table. With the increase in temperature, it was found that R^2 first decreased and then increased which was consistent with the other models, but the K_{YN} value showed a consistent increase with the increase in temperature and τ value showed a consistent decrease with increase in temperature. The K_{YN} values showed a regular increase with increase in concentration and τ value showed a regular decrease which was consistent with the experimental data. K_{YN} value for the change in the pH was found to increase drastically and the τ value seemed to decrease. The τ value for the change in pH was found to be inconsistent with the experimental data. With increase in the bed height, correlation coefficient was found to decrease for all concentrations and the τ value was found to increase. The τ value was mostly consistent with the experimental data for all the concentrations.

Wolborska model

The BTC was fitted with Wolborska model also which was showed in the plot of $\ln\left(\frac{C}{C_o}\right)$ vs t. Table 4 gives the Wolborska parameters. It was found that kinetic coefficient (β_a) was decreased with increase in concentration but the adsorption capacity N_o increased. The increase in adsorption capacity could be attributed due to the fact that increase in the probability of adsorption was owing to increased concentration of MB. With the increase in flow rate, it was found that β_a was found to increase and adsorption capacity was found to be stable without any variation. With the change in pH, it was found that β_a got reduced compared with the neutral pH and adsorption capacity was also found to reduce, but increase in temperature showed a decrease in β_a and then later increased, while adsorption capacity decreased. With the increase in bed height, β_a was found to decrease, while N_o increased because of the increase in the adsorption sites.

BDST model

BDST model was obtained by plotting bed height vs time for C/C_o values of 0.02 and 0.5 and Fig.S2 (a), (b) represents, the straight line while the BDST parameters were presented in Table S3 for BTC at a different concentrations at a pH of 6.9, temperature 303 K and a flow rate of 3.5 ml min^{-1}. The R^2 obtained was found to be nearly 1 for all the concentrations for C/C_o of 0.02 except for 200 mg/L which showed a value of 0.908, this suggested that BTC fitted well with $C/C_{o-} = 0.02$. From the table, it can be inferred that with the increase in concentration there was no regular change in K_a, N_o and R^2. $C/C_o = 0.5$ also showed a good fit to BSDT model except for 200 mg/L which showed a poorer fit at $C/C_o = 0.02$. The value of adsorption capacity was found to increase with increase in concentration whereas, K_a value showed no regular trend. BTC was found to follow BDST in most of the concentrations, whereas, Thomas model was also found to be followed at higher flow rate. The CGLAC was compared with other adsorbents with removal of different adsorbates, with column parameters and fitted models are shown in Table 5.

ANN and ANFIS modeling

ANN and ANFIS predictions for the removal of MB by the activated carbon were carried out. Five variables such as concentration, pH, temperature, bed height and flow rates were used to predict the output in both the models and the removal of MB by the activated carbon were the response that was predicted. The discussion on the theory of ANN can be seen elsewhere [51- 53]. Totally, 60 experiments were carried out for the prediction using ANN and ANFIS network, out of which the data of 40 experiments were used for training purposes and 20 experiments were used for prediction purpose. A concentration range from100 to 500 mg/L, pH range between 2 to 10, temperature range from 303 to 333 K, flow rate between 3.5 to 6.5 ml min^{-1} and bed height range of 1 to 2 cm were taken as input to the ANN and ANFIS model. Extensive literature survey has shown that only very limited work has been done for ANN prediction in the bed column removal of MB, but most of the work was not carried out with percentage removal of MB and ANFIS modeling was also not found.

So, in this work, both the models were compared by the correlation coefficient of the predicted data and experimental data. Fig. S3 (a, c) shows the linear plot of the predicted and experimental data for ANN and ANFIS. ANN model with feed forward back propagation method was carried out with Trainlm as training function, learngdm as adaption learning function and MSE was used to minimize the error [54]. Number of neurons was fixed at 10 after carrying out the model with a different number

Table 5: Comparison of column models by various adsorbent and adsorbate.

	Adsorbent	Adsorbate	Parameters	Column models	Best model	References
1	Peanut Husk biomass	Yellow BG	Initial concentration flow rate, bed height	Thomas, BTC, BDST	Thomas	[48]
2	*Eucalyptussheathiana* bark biomass	MB	Initial concentration pH, flow rate, bed height	Thomas, BDST	Thomas	[49]
3	Hyacinth root	Lead	Initial concentration pH, flow rate, bed height	Thomas, BTC, Yoon	Thomas	[55]
4	Sunflower shells	Copper	Initial concentration pH, flow rate, bed height	Thomas, Adams - Bohart and Yoon	Thomas	[56]
5	*Auricularia* matrix Waste	Lead	pH, flow rate and bed height	Thomas and Adams - Bohart	Thomas	[57]
6	Watermelon rind	MB	Initial concentration flow rate and bed height	Thomas, Adams Bohart and BDST	Thomas	[58]
7	CGLAC	MB	Initial concentration flow rate, pH and bed height	Thomas , Adams Bohart, BDST, BTC, Wolborska and Yoon	BTC, BDST and Thomas	This study

of neurons and it was found that the minimum error occurred only with a number of a neuron as 10. The transfer function, Tansig gave the best result compared to logsig or pureln. In ANFIS membership type of Gbelmf was taken as it gave best results compared to the other membership functions and a number of membership functions were fixed at 4. The number of epochs for both ANN and ANFIS were fixed at 1000. The ANN data was showed the R^2 values are 0.947 and 0.92 for the training and validation data. ANFIS model showed the value of R^2 as 1.0 and 0.960 for training and validation data respectively. Both the models were found to be applicable to the removal of MB by the activated carbon as the correlation coefficient value was above 0.9 for both the training and validation data. However, ANFIS model showed excellent correlation with the experimental data which could be inferred from Fig. S3 (b, d) and R^2 value.

CONCLUSIONS

In this study, the inexpensive, abundantly available plant leaves of *Calotropis Gigantea* activated carbon were used as an alternative to commercial adsorbent for the removal of MB from industrial wastewater. The CGLAC was characterized by SEM, FT-IR, XRD, Raman, TGA/DTA, EDAX, BET, TGA/DTA and XPS. These experimental analyses widely explained the physical properties and adsorption performance of CGLAC. The column study was used to test the effect of dynamic column parameters such as, initial concentration, bed height, pH, flow rate and temperature for the removal of MB. The experimental data was applied to column models like Thomas model, Adams-Bohart model, Wolbroska model, Yoon-Nelson model and BDST model. The BTCs were determined at different flow rates, initial concentrations, bed heights and temperatures from 303 to 333 K. The obtained results indicated that the removal of MB were strongly dependent on bed depth, flow rate and initial concentration. An increase in bed height resulted in improved adsorption performance. With the increase in flow rates, the adsorption capacity was found to decrease. The results of the removal of MB by CGLAC using column method showed that removal percentage increased with the increase in bed height. With the increase in flow rate, concentration and temperature, the removal of the dye decreased and also neutral pH was found to be ideal. Out of various models that were investigated for BTC, BDST model was found to fit the best for the experimental data, then followed by Thomas model. Though, the non - linear models such as ANN and ANFIS gave an excellent prediction, ANFIS was found to fit better for the prediction of removal of the dye by the column bed.

This work indicated that the good adsorption capacity and acceptability of extensively used Thomas, Yoon–Nelson and BDST column models make the *Calotropis Gigantea* leaves activated carbon, gorgeous, excellent and novel adsorbent for treating dyes and heavy metals in industrial wastewater. This work would be both cost - free and eco-friendly.

Conflicts of interest

Authors declared that they have no conflicts of interest.

Acknowledgments

The first author gratefully acknowledges the All India Council for Technical Education (AICTE) for providing

funding under Technical Education Quality Improvement Programme (TEQIP) phase -II scholarship scheme and Prof. R. Sharmil Suganya for her valuable contribution and suggestion for the research work.

Received : Apr. 7, 2019 ; Accepted : Sep. 2, 2019

REFERENCES

[1] Kumar P.S., Deepthi A.S., Bharani R, Rakkesh, G., Study of Adsorption of Cu (II) Ions from Aqueous Solution by Surface-Modified Eucalyptus Globulus Seeds in a Fixed-Bed Column: Experimental Optimization and Mathematical Modeling, *Res. on Chem. Interms.*, **41(11)**: 8681-8688 (2015).

[2] Ayuba S., Mohammadib A.A., Yousefi M., Changanic F., Performance Evaluation of Agro-Based Adsorbents for the Removal of Cadmium from Wastewater, *Desalination And Water Treatment.*, **142**: 293-299 (2019).

[3] Dehghani M.H., Zarei A., Yousefi M., Efficiency of Ultrasound for Degradation of an Anionic Surfactant from Water: Surfactant Determination Using Methylene Blue Active Substances Method, *Methodsx.*, **6**: 805-814 (2019).

[4] Jawad A.H., Mohammed S.A., Mastuli M.S., Abdullah M.F., Carbonization of Corn (Zea Mays) Cob Agricultural Residue by One-Step Activation with Sulfuric Acid for Methylene Blue Adsorption, *Desalination and Water Treatment.*, **118**: 342-351 (2018).

[5] Rashid R.A., Jawad A.H., Azlan M., Ishak M., Kasim N.N., $Fecl_3$-Activated Carbon Developed from Coconut Leaves: Characterization and Application for Methylene Blue Removal, *Sains Malaysiana.*, **47(3)**: 603-610 (2018).

[6] Gupta V.K., Tyagi I., Agarwal S., Singh R., Chaudhary M., Harit A., Kushwaha S., Column Operation Studies for the Removal of Dyes and Phenols Using a Low Cost Adsorbent. *Global J of Environ Sci and Manag.*, **2(1)**: 1-10 (2016).

[7] Saleh H.N., Dehghani M.H., Nabizadeh R., Mahvi A.H., Hossein F., Ghaderpoori M., Yousefi M., Mohammadi A.,. Data on the Acid Black 1 Dye Adsorption From Aqueous Solutions by Low-Cost Adsorbent-Cerastoderma Lamarcki Shell Collected from the Northern Coast of Caspian Sea, *Data in Brief.*, **17**: 774-780 (2018).

[8] Ali H., Jawada R., Razuana Jimmy Nelson Appaturib., Lee D. Wilsonc., Adsorption And Mechanism Study for Methylene Blue Dye Removal with Carbonized Watermelon (Citrullus Lanatus) Rind Prepared *via* One-Step Liquid Phase H_2SO_4 Activation, *Surfaces And Interfaces.*, **16**: 76–84 (2019).

[9] Reddy P.M., Subrahmanyam C., Green Approach for Wastewater Treatment Degradation and Mineralization of Aqueous Organic Pollutants by Discharge Plasma, *I & E Chem Rese*., **51(34)**: 11097-11103 (2012).

[10] Jawada A.H., Mallahb S.H., Mastulia M.S., Adsorption Behavior of Methylene Blue on Acid-Treated Rubber (Hevea Brasiliensis) Leaf, *Desalination And Water Treatment.*, **124**: 297-307 (2018).

[11] Yousefi M., Nabizadeh R., Alimohammadi M., Mohammadi A.A., Mahvi A.H., Removal of Phosphate From Aqueous Solutions Using Granular Ferric Hydroxide Process Optimization by Response Surface Methodology, *Desalination and Water Treatment.*, **158**: 290-300 (2019).

[12] Jawad A.H., Sauodi M.H., Mastuli M.S., Aouda M.A., Radzun K.A., Pomegranate Peels Collected from Fresh Juice Shop as a Renewable Precursor for High Surface Area Activated Carbon with Potential Application for Methylene Blue Adsorption, *Desalination and Water Treatment.*, **124**: 287-296 (2018).

[13] Mohammadi A.A., Zarei A., Alidadi H., Afsharnia M., Shams M., Two-Dimensional Zeolitic Imidazolate Framework-8 for Efficient Removal of Phosphate From Water, Process Modeling, Optimization, Kinetic, and Isotherm Studies, *Desalination and Water Treatment.*, **129**: 244-254 (2018).

[14] Jawad A.H., Carbonization of Rubber (Hevea Brasiliensis) Seed Shell by One-Step Liquid Phase Activation with H_2SO_4 for Methylene Blue Adsorption, *Desalination and Water Treatment.*, **129**:279-288 (2018).

[15] Farasati M., Haghighi S., Boroun S., Cd Removal From Aqueous Solution Using Agricultural Wastes, *Desalination and Water Treatment.*, **57(24)**: 11162-11172 (2016).

[16] Farzia S., Farasatib M., Bansoulehc B.F., Pirsahebd M., Evaluation of Batch and Continuous Adsorption Kinetic Models of Cadmium from Aqueous Solutions Using Sugarcane Straw Nano-Structure Absorbent, *Desalination and Water Treatment.*, **115**: 135-144 (2018).

[17] Jawad A.H., Ngoh Y.S., Radzun K.A., Utilization of Watermelon (Citrullus Lanatus) Rinds as a Natural Low-Cost Biosorbent for Adsorption of Methylene Blue: Kinetic, Equilibrium and Thermodynamic Studies, *Journal of Taibah University for Science*., **12(4)**: 371-381 (2018).

[18] Jawad A.H., Rashid R.A., Ishak M.A.M., Ismail K., Adsorptive Removal of Methylene Blue by Chemically Treated Cellulosic Waste Banana (Musa Sapientum) Peels, *Journal of Taibah University for Science.*, **12(6)**: 809-819 (2018).

[19] Thomas H.C., Heterogeneous Ion Exchange in a Flowing System, *Am. Chem. Soci.*, **66(10)**: 1664 (1944).

[20] Yoon Y.H., Nelson J.H., Application of Gas Adsorption Kinetics I. A Theoretical Model for Respirator Cartridge Service Life, *Am. Ind. Hyg. Assoc. J.*, **45(8)**: 509- (1984).

[21] Sharma R., Singh B., Removal Of Ni (II) Ions from Aqueous Solutions Using Modified Rice Straw in a Fixed Bed Column, *Bio Techn.*, **146**: 519- (2013).

[22] Zubrik A., Matik M., Hredzák S., Lovás M., Danková Z., Kováčová M., Briančin J., Preparation of Chemically Activated Carbon from Waste Biomass by Single-Stage and Two-Stage Pyrolysis, *J. of Clean. Prod*., **143**: 643-653 (2017).

[23] Goswami M., Phukan P., Enhanced Adsorption of Cationic Dyes Using Sulfonic Acid Modified Activated Carbon, *J. of Environ. Chem. Eng.*, **5(4)**: 3508-3517 (2017).

[24] Mudyawabikwa B., Mungondori H.H., Tichagwa L. Katwire D.M., Methylene Blue Removal Using a Low-Cost Activated Carbon Adsorbent from Tobacco Stems: Kinetic and Equilibrium Studies, *Wat. Sci. and Techn.*, (2017).

[25] Tahiruddin N.S.M., Ab Rahman S.Z., Adsorption of Lead In Aqueous Solution by a Mixture of Activated Charcoal and Peanut Shell, *World J. Sci. Technol. Res.*, **1**:102- (2013).

[26] Sounthararajah D.P., Loganathan P., Kandasamy J., Vigneswaran S., Adsorptive Removal of Heavy Metals from Water Using Sodium Titanate Nanofibres Loaded onto GAC in Fixed-Bed Columns, *J. Hazard. Mater.*, **287**: 306-316 (2015).

[27] Sayğılı H., Güzel F., High Surface Area Mesoporous Activated Carbon from Tomato Processing Solid Waste by Zinc Chloride Activation: Process Optimization, Characterization and Dyes Adsorption, *J. of Clean Prod.*, **113**: 995-1004 (2016).

[28] Wu A., Yan J., Xu W., Li X., Fabrication of Waste Biomass Derived Carbon by Pyrolysis, *Mater. Let*., **73**: 60-63 (2016).

[29] Islam M.A., Ahmed M.J., Khanday W.A., Asif M., Hameed B.H., Mesoporous Activated Carbon Prepared from NaOH Activation of Rattan (Lacosperma Secundiflorum) Hydrochar for Methylene Blue Removal, *Ecotoxi and Environ Saf.*, **138**: 279-285 (2017).

[30] Lu Y., Yu J., Cheng S., Magnetic Composite of Fe3O4 and Activated Carbon as an Adsorbent for Separation of Trace Sr(II) from Radioactive Wastewater, *Journal of Radio and Nucl. Chem.*, **30(3)**: 2371-2377 (2015).

[31] Andreoli E., Barron A.R., CO_2 Adsorption by Para-Nitroaniline Sulfuric Acid-Derived Porous Carbon Foam, *Carbon.*, **2(4)**: 25 (2016).

[32] Saranya P., Ranjitha S., Sekaran G., Immobilization of Thermotolerant Intracellular Enzymes on Functionalized Nanoporous Activated Carbon and Application To Degradation of an Endocrine Disruptor: Kinetics, Isotherm and Thermodynamics Studies, *RSC Adv.*, **5(81)**:66239-66259 (2015).

[33] Obregón-Valencia D., Del Rosario Sun-Kou M., Comparative Cadmium Adsorption Study on Activated Carbon Prepared From Aguaje (Mauritia Flexuosa) and Olive Fruit Stones (Olea Europaea L), *J. Environ. Chem. Eng.*, **2(4)**: 2280-2288 (2014).

[34] Tavares A.P., Silva C.G., Dražić G., Silva A.M., Loureiro J.M., Faria J.L., Laccase Immobilization over Multi-Walled Carbon Nanotubes: Kinetic, Thermodynamic and Stability Studies, *Journ of Colld and Inter Sci.*, **454**: 52-60 (2015).

[35] De Oliveira G.F., De Andrade R.C., Trindade M.A.G., Andrade H.M.C., De Carvalho C.T., Thermogravimetric and Spectroscopic Study (TG–DTA/FT–IR) of Activated Carbon from the Renewable Biomass Source Babassu., *Quím Nova.*, **40(3)**: 284 (2017).

[36] Arsyad N.A.S., Razab M.K.A.A., Noor A.M., Amini M.H.M., Yusoff N.N.A.N., Halim A.Z.A., Yusuf N.A.A.N., Masri M.N., Sulaiman M.A., Abdullah N.H., Effect of Chemical Treatment on Production of Activated Carbon from Cocos Nucifera L.(Coconut) Shell by Microwave Irradiation Method, *J. Trop. Resour. Sustain. Sci*., **4**: 112- (2016).

[37] Yorgun S., Yıldız D., Preparation and Characterization of Activated Carbons from Paulownia Wood by Chemical Activation with H_3PO_4, *J. of the Taiw. Inst. Chem. Eng.*, **53**: 122-131 (2015).

[38] Zuim D.R., Carpiné D., Distler G.A.R., De Paula Scheer A., Igarashi-Mafra L., Mafra M.R., Adsorption of Two Coffee Aromas from Synthetic Aqueous Solution onto Granular Activated Carbon Derived from Coconut Husks, *J. of Food Eng.*, **104(2)**: 284-292 (2011).

[39] Hassan A.F., Youssef A.M., Priecel P., Removal of Deltamethrin Insecticide over Highly Porous Activated Carbon Prepared from Pistachio Nutshells, *Carbon Letters.*, **14(4)**: 234- (2017).

[40] Zhang Z., Luo X., Liu Y., Zhou P., Ma G., Lei Z., Lei L., A Low Cost And Highly Efficient Adsorbent (Activated Carbon) Prepared from Waste Potato Residue, *J. of the Tai Ins. of Chem. Eng.*, **49**: 206-211 (2015).

[41] Chandane V., Singh V.K., Adsorption of Safranin Dye from Aqueous Solutions Using a Low-Cost Agro-Waste Material Soybean Hull, *Des and Wat Treat.*, **57(9)**: 4122-4134 (2016).

[42] Finol J., Guo Y.K., Jing X.D., A Rule Based Fuzzy Model for the Prediction of Petrophysical Rock Parameters, *J. of Petro. Sci. and Eng.*, **29(2)**: 97-113 (2001).

[43] Ghosh A., Das P., Sinha, K., Modeling of Biosorption of Cu (II) By Alkali-Modified Spent Tea Leaves using Response Surface Methodology (RSM) and Artificial Neural Network (ANN), *App Wat Sci.*, **5(2)**: 191-199 (2015).

[44] Badkar D.S., Pandey K.S., Buvanashekaran G., Development of RSM-and ANN-Based Models to Predict and Analyze the Effects of Process Parameters of Laser-Hardened Commercially Pure Titanium on Heat Input and Tensile Strength, *The Int. J. of Adv. Manuf. Tech.*, **65(9-12)**: 1319-1338 (2013).

[45] Nayak A.K., Pal A., Green and Efficient Biosorptive Removal of Methylene Blue by Abelmoschus Esculentus Seed: Process Optimization and Multi-Variate Modeling, *J. of Environ. Manage.*, **200**:145-159 (2017).

[46] Sugeno M., Kang G.T., Structure Identification of Fuzzy Model, *Fuz Sets and Sys.*, **28(1)**: 15-33 (1988).

[47] Meshalkin V.P., Bol'shakov A.A., Petrov D.Y., Krainov O.A., Algorithms and Software System for Controlling the Quality of Glass Batch Using Artificial Neural Networks, *Theo. Found. Chem. Eng.*, **46(3)**: 284-287 (2012).

[48] Sadaf S., Bhatti H.N., Batch and Fixed bed Column Studies for the Removal of Indosol Yellow BG Dye by Peanut Husk, *Journal of the Tai Inst. of Chem. Eng.*, **45(2)**: 541-553 (2014).

[49] Afroze S., Sen T.K., Ang H.M., Adsorption Performance of Continuous Fixed Bed Column for the Removal of Methylene Blue (MB) Dye Using Eucalyptussheathiana Bark Biomass, *Research on Chemical Intermediates.*, **42(3)**: 2343-2364 (2016).

[50] Maeda C.H., Araki C.A., Moretti A.L., De Barros M.A.S.D., Arroyo P.A., Adsorption and Desorption Cycles of Reactive Blue BF-5G Dye in a Bone Char Fixed-Bed Column, *Environmental Science and Pollution Research.*, 1-10 (2018).

[51] Shahriari S., Atashrouz S., Pazuki G., Mathematical Model of the Phase Diagrams of Ionic Liquids-Based Aqueous Two-Phase Systems Using the Group Method of Data Handling and Artificial Neural Networks, *Theo. Found. Chem. Eng.*, **52(1)**: 146-155 (2018).

[52] Kasiri M.B., Aleboyeh H., Aleboyeh A., Modeling and Optimization of Heterogeneous Photo-Fenton Process with Response Surface Methodology and Artificial Neural Networks, *Environ. Sci. & Techn.*, **42**(21): 7970-7975 (2008).

[53] Aber S., Amani-Ghadim A.R., Mirzajani V., Removal of Cr (VI) From Polluted Solutions by Electrocoagulation: Modeling of Experimental Results Using Artificial Neural Network, *J. Hazard. Mater.*, **171(1-3):** 484-490 (2009).

[54] Kayak O., Zadeh L.A., "Fuzzy Inference Systems: A Critical Review, Computational Intelligence Soft Computing and Fuzzy-Neurointegration with Applications", Springer, Berlin, Heidelberg. (1998).

[55] Mitra T., Singha B., Bar N., Das S.K., Removal of Pb (II) Ions from Aqueous Solution Using Water Hyacinth Root by Fixed-Bed Column and ANN Modeling, *Journal of Hazardous Materials.*, **273**: 94-103 (2014).

[56] Oguz E., Ersoy M., Removal of Cu^{2+} from Aqueous Solution by Adsorption in A Fixed Bed Column and Neural Network Modelling, *Chemical Engineering Journal.*, **164(1)**: 56-62 (2010).

[57] Qu J., Song T., Liang J., Bai X., Li Y., Wei Y., Huang S., Dong L., Jin Y., Adsorption of Lead (II) From Aqueous Solution by Modified Auricularia Matrix Waste: A Fixed-Bed Column Study., *Ecotoxicology and Environmental Safety*., **169**: 722-729 (2019).

[58] Lakshmipathy R., Sarada NC., Methylene Blue Adsorption onto Native Watermelon Rind: Batch and Fixed Bed Column Studies, *Desalination Water Treat.*, **57(23)**: 10632–10645 (2016).